VISCOUS COMPUTATION AND DESIGN OF OPTIMAL AERODYNAMIC CONFIGURATIONS IN SUPERSONIC FLOW

by Adriana Nastase

Lehrgebiet Aerodynamik des Fluges

Rheinisch - Westfälische Technische Hochschule Aachen, Germany

Abstract In this paper some new, original spectral solutions for the three-dimensional stationary, laminar, compressible boundary layer equations on flattened flying configurations in supersonic flow are obtained. The most important applications of these spectral solutions are the computation of the total drag coefficient $C_d^{(t)}$, including the friction effect and the performing of viscous optimal design of the shapes of the flying configurations via iterative optimum-optimorum theory of the author. The chosen configuration for the exemplification of the theory is the delta wing alone.

1. The Edge Solution of the Boundary Layer

Let us refer the thick, lifting delta wing with subsonic leading edges, with the similarity parameter of planprojection $\nu=B\ell$ ($B=\sqrt{M_\infty^2-1}$, $\ell=\ell_1/h_1$ with ℓ_1 the half span, h_1 the maximal depth, M_∞ the cruising Mach number) to a three-orthogonal system of coordinates $Ox_1x_2x_3$ having the apex of the wing O as vertex. The Ox_1-Axis has the direction of the shockfree entrance. The undisturbed velocity $\vec{v}_\infty$ is parallel to the symmetry plane Ox_1x_3. The downwashes w and w^* of the thin and thick-symmetrical wing components are given in the form of superpositions of homogeneous polynomes in $\tilde{x}_1$ and $\tilde{x}_2$ i.e.:

$$w = \sum_{m=1}^{N} \tilde{x}_1^{m-1} \sum_{k=0}^{m-1} \tilde{w}_{m-k-1,k} \, |\tilde{y}|^k \qquad (1a)$$

$$w^* = \sum_{m=1}^{N} \tilde{x}_1^{m-1} \sum_{k=0}^{m-1} \tilde{w}^*_{m-k-1,k} \, |\tilde{y}|^k. \qquad (1b)$$

The corresponding axial disturbance velocities u and u^* for the delta wing components with subsonic leading edges, as in [1]-[7] for the outer inviscid flow are

$$u = \ell \sum_{n=1}^{N} \tilde{x}_1^{n-1} \left\{ \sum_{q=0}^{E(\frac{n}{2})} \frac{\tilde{A}_{n,2q} \, \tilde{y}^{2q}}{\sqrt{1-\tilde{y}^2}} + \sum_{q=1}^{E(\frac{n-1}{2})} \tilde{C}_{n,2q} \, \tilde{y}^{2q} \cosh^{-1}\sqrt{\frac{1}{\tilde{y}^2}} \right\} \qquad (2)$$

$$u^* = \ell \sum_{n=1}^{N} \tilde{x}_1^{n-1} \left\{ \sum_{q=0}^{E(\frac{n-2}{2})} \tilde{D}^*_{n,2q} \, \tilde{y}^{2q} \sqrt{1-\nu^2\tilde{y}^2} + \sum_{q=0}^{n-1} \tilde{H}^*_{nq} \, \tilde{y}^q \left[\cosh^{-1}M_1 + (-1)^q \cosh^{-1}M_2 \right] + \sum_{q=1}^{E(\frac{n-1}{2})} \tilde{C}^*_{n,2q} \, \tilde{y}^{2q} \cosh^{-1}\sqrt{\frac{1}{\nu^2 \, \tilde{y}^2}} \right\}. \qquad (3)$$

Here is $\tilde{x}_1 = x_1/h_1$, $\tilde{x}_2 = x_2/\ell_1$, $\tilde{x}_3 = x_3/h_1$, $\nu = B\ell$, $B = \sqrt{M_\infty^2 - 1}$, $\ell = \ell_1/h_1$, $\tilde{y} = \tilde{x}_2/\tilde{x}_1$, $w = \tilde{w}$, $w^* = \tilde{w}^*$, $u = \ell\,\tilde{u}$, $u^* = \ell\,\tilde{u}^*$ and

$$M_1 = \sqrt{\frac{(1+\nu)(1-\nu\tilde{y})}{2\nu\,(1-\tilde{y})}}, \tag{4a}$$

$$M_2 = \sqrt{\frac{(1+\nu)(1+\nu\tilde{y})}{2\nu\,(1+\tilde{y})}}. \tag{4b}$$

The coefficients $\tilde{A}_{n,2q}$, $\tilde{C}_{n,2q}$ of $\tilde{u}$ and $\tilde{H}^*_{nq}$, $\tilde{D}^*_{n,2q}$, $\tilde{C}^*_{n,2q}$ of $\tilde{u}^*$ and the coefficients $\tilde{w}_{ij}$, $\tilde{w}^*_{ij}$ of the downwashes $\tilde{w}$ and, respectively $\tilde{w}^*$ are related through the following linear and homogeneous relations as in [1], [5], [13] i.e.

$$\tilde{A}_{n,2q} = \sum_{j=0}^{n-1} \tilde{a}^{(n)}_{2q,j}\ \tilde{w}_{n-j-1,j},$$

$$\tilde{C}_{n,2q} = \sum_{j=0}^{n-1} \tilde{c}^{(n)}_{2q,j}\ \tilde{w}_{n-j-1,j} \tag{5a,b}$$

$$\tilde{H}^*_{nq} = \sum_{j=0}^{n-1} \tilde{h}^{*(n)}_{qj}\ \tilde{w}^*_{n-j-1,j},$$

$$\tilde{D}^*_{n,2q} = \sum_{j=0}^{n-1} \tilde{d}^{*(n)}_{2q,j}\ \tilde{w}^*_{n-j-1,j},$$

$$\tilde{C}^*_{n,2q} = \sum_{j=0}^{n-1} \tilde{c}^{*(n)}_{2q,j}\ \tilde{w}^*_{n-j-1,j}. \tag{6a-c}$$

The coefficients $\tilde{a}^{(n)}_{2q,j}$, $\tilde{c}^{(n)}_{2q,j}$, $\tilde{h}^{*(n)}_{qj}$, $\tilde{d}^{*(n)}_{2q,j}$, $\tilde{c}^{*(n)}_{2q,j}$ are non-linear functions depending only on ν. The inviscid drag coefficients C_d, C_d^* of the thin and thick-symmetrical delta wing components are:

$$C_d = 8\,\ell \int_{\tilde{0}\tilde{A}_1\tilde{C}} \tilde{u}\,\tilde{w}\,\tilde{x}_1\,d\tilde{x}_1\,d\tilde{y}, \tag{7a}$$

$$C_d^* = 8\,\ell \int_{\tilde{0}\tilde{A}_1\tilde{C}} \tilde{u}^*\,\tilde{w}^*\,\tilde{x}_1\,d\tilde{x}_1\,d\tilde{y}. \tag{7b}$$

Let us now denote $\tilde{\delta}^+$ and $\tilde{\delta}^-$ the dimensionless thicknesses of the boundary layers on the upper and lower surfaces ($\tilde{\delta}^+ = \delta^+/h_1$, $\tilde{\delta}^- = \delta^-/h_1$) of the thick, lifting delta wing (Fig.1). An easy matching of these zonal solutions is obtained if the slopes of boundary layer thicknesses $\tilde{\delta}^+$ and $\tilde{\delta}^-$ in the Ox_3 direction are approximated in form of superpositions of homogeneous polynomes in $\tilde{x}_1$ and $\tilde{x}_2$ as in [8], [9] i.e.

$$\frac{\partial\tilde{\delta}^+}{\partial\tilde{x}_1} = \sum_{m=1}^{N} \tilde{x}_1^{m-1} \sum_{k=0}^{m-1} \tilde{\delta}^+_{m-k-1,k}\ |\tilde{y}|^k \tag{8a}$$

$$\frac{\partial\tilde{\delta}^-}{\partial\tilde{x}_1} = \sum_{m=1}^{N} \tilde{x}_1^{m-1} \sum_{k=0}^{m-1} \tilde{\delta}^-_{m-k-1,k}\ |\tilde{y}|^k. \tag{8b}$$

The modified downwashes $\tilde{w}_1$ and $\tilde{w}_1^*$ at the edge of the upper boundary layer are of the following form:

$$\tilde{w}_1 = \sum_{m=1}^{N} \tilde{x}_1^{m-1} \sum_{k=0}^{m-1} \tilde{w}^{(1)}_{m-k-1,k}\ |\tilde{y}|^k \tag{9a}$$

$$\tilde{w}_1^* = \sum_{m=1}^{N} \tilde{x}_1^{m-1} \sum_{k=0}^{m-1} \tilde{w}^{*(1)}_{m-k-1,k}\ |\tilde{y}|^k. \tag{9b}$$

The modified coefficients in these formulas of $\tilde{w}_1$ and $\tilde{w}_1^*$ are

$$\tilde{w}^{(1)}_{ij} = \tilde{w}_{ij} + \frac{1}{2}\,(\tilde{\delta}^+_{ij} + \tilde{\delta}^-_{ij}), \tag{10a}$$

$$\tilde{w}^{*(1)}_{ij} = \tilde{w}^*_{ij} + \frac{1}{2}\,(\tilde{\delta}^+_{ij} - \tilde{\delta}^-_{ij}). \tag{10b}$$

The axial disturbance velocities u_1 and u_1^* at the edge of the boundary layer are obtained from the formulas (2) and (3) by replacing in (1a,b)-(6a-c) the coefficients $\tilde{w}_{ij}$, $\tilde{w}^*_{ij}$ with the modified coefficients $\tilde{w}^{(1)}_{ij}$, $\tilde{w}^{*(1)}_{ij}$. The inviscid axial velocities u_e^+ and u_e^- at the edges of the upper and lower boundary layers are obtained from u_1 and u_1^* as follows

$$u_e^+ = - u_1 + u_1^* \ , \ u_e^- = u_1 + u_1^* \qquad (11)$$

2. Spectral Solutions for the Three-Dimensional, Compressible, Boundary Layer

The starting points for these spectral solutions are the continuity, the impulse, the physical equation of state and the energy equations as in [16]-[21] i.e.

- The continuity equation:

$$\frac{\partial(\varrho u)}{\partial x_1} + \frac{\partial(\varrho v)}{\partial x_2} + \frac{\partial(\varrho w)}{\partial x_3} = 0 \qquad (12)$$

- The impulse equations:

$$u \frac{\partial u}{\partial x_1} + v \frac{\partial u}{\partial x_2} + w \frac{\partial u}{\partial x_3} = \frac{1}{\varrho} \left\{ \frac{\partial p_e}{\partial x_1} + \frac{\partial}{\partial x_1} \left[\mu \left(2 \frac{\partial u}{\partial x_1} - \frac{2}{3} \operatorname{div} \vec{v} \right) \right] + \frac{\partial}{\partial x_2} \left[\mu \left(\frac{\partial u}{\partial x_2} + \frac{\partial v}{\partial x_1} \right) \right] + \frac{\partial}{\partial x_3} \left[\mu \frac{\partial w}{\partial x_1} \right] \right\}$$

$$u \frac{\partial v}{\partial x_1} + v \frac{\partial v}{\partial x_2} + w \frac{\partial v}{\partial x_3} = \frac{1}{\varrho} \left\{ - \frac{\partial p_e}{\partial x_2} + \frac{\partial}{\partial x_2} \left[\mu \left(2 \frac{\partial v}{\partial x_2} - \frac{2}{3} \operatorname{div} \vec{v} \right) \right] + \frac{\partial}{\partial x_3} \left[\mu \frac{\partial w}{\partial x_2} \right] + \frac{\partial}{\partial x_1} \left[\mu \left(\frac{\partial u}{\partial x_2} + \frac{\partial v}{\partial x_1} \right) \right] \right\}$$

$$u \frac{\partial w}{\partial x_1} + v \frac{\partial w}{\partial x_2} + w \frac{\partial w}{\partial x_3} = \frac{1}{\varrho} \left\{ \frac{\partial}{\partial x_1} \left[\mu \frac{\partial w}{\partial x_1} \right] + \frac{\partial}{\partial x_2} \left[\mu \frac{\partial w}{\partial x_2} \right] \right\} \qquad (13a\text{-}c)$$

- The energy equation and the physical gas equation for perfect gas :

$$\varrho \left\{ u \frac{\partial e}{\partial x_1} + v \frac{\partial e}{\partial x_2} + w \frac{\partial e}{\partial x_3} \right\} = -p_e \operatorname{div} \vec{v} + \lambda \Delta_3 T + \mu \phi \ , \ p = \varrho R T \qquad (14a,b)$$

$$\phi = 2 \left[\left(\frac{\partial u}{\partial x_1} \right)^2 + \left(\frac{\partial v}{\partial x_2} \right)^2 + \left(\frac{\partial w}{\partial x_3} \right)^2 \right] + \left(\frac{\partial w}{\partial x_1} \right)^2 + \left(\frac{\partial w}{\partial x_2} \right)^2 + \left(\frac{\partial v}{\partial x_1} + \frac{\partial u}{\partial x_2} \right)^2 - \frac{2}{3} \left(\operatorname{div} \vec{v} \right)^2 ,$$

$$e = T + \frac{1}{2} (u^2 + v^2 + w^2).$$

Hereby is T the absolute temperature, ϕ the dissipation function, e the internal energy. Let us further introduce the coordinate $\eta = (x_3 - Z^+(x_1,x_2))/\delta^+(x_1,x_2)$ in the upper boundary layer. The dimensionless axial, lateral and vertical velocities u_δ, v_δ, w_δ on the upper boundary layer are

$$u_\delta = u_e \sum_{i=1}^{N} u_i \eta^i \ , \ v_\delta = v_e \sum_{i=1}^{N} v_i \eta^i \ ,$$

$$w_\delta = w_e \sum_{i=1}^{N} w_i \eta^i \qquad (15a\text{-}c)$$

$$(u_e = u_e^+ \ , \ v_e = v_e^+ \ , \ w_e = w_e^+) \ .$$

Here u_e, v_e, w_e are the edge values, obtained from the outer potential flow. The non-slip conditions at $\eta = 0$, $u_\delta = v_\delta = w_\delta = 0$ on the surface of the wing are automatically satisfied. The matching conditions with the potential flow at the edge of the boundary layer ($\eta \cong 1$) are

$$u_\delta = u_e \ , \quad \frac{\partial u_\delta}{\partial \eta} = 0 \quad (\tau_{x_1} = 0)$$

$$\frac{\partial^2 u_\delta}{\partial \eta^2} = 0 \quad \left(\frac{\partial \tau_{x_1}}{\partial \eta} = 0 \right) , \qquad (16a\text{-}c)$$

$$v_\delta = v_e \ , \quad \frac{\partial v_\delta}{\partial \eta} = 0 \quad (\tau_{x_2} = 0)$$

$$\frac{\partial^2 v_\delta}{\partial \eta^2} = 0 \quad \left(\frac{\partial \tau_{x_2}}{\partial \eta} = 0 \right) . \qquad (17a\text{-}c)$$

These boundary layer conditions lead to the following linear and homogeneous relations among the coefficients u_i, v_i, w_i of u_δ , v_δ and w_δ

$$\sum_{i=1}^{N} u_i = 1 \quad , \quad \sum_{i=1}^{N} i\, u_i = 0$$

$$\sum_{i=1}^{N} i\,(i-1)\, u_i = 0 \quad , \qquad (18a\text{-}c)$$

$$\sum_{i=1}^{N} v_i = 1 \quad , \quad \sum_{i=1}^{N} i\, v_i = 0 \ ,$$

$$\sum_{i=1}^{N} i\,(i-1)\, v_i = 0 \quad . \qquad (19a\text{-}c)$$

For laminar flow at the edge ($\eta = 1$)

$$w_\delta = w_e \quad \text{i.e.} \quad \sum_{i=1}^{N} w_i = 1 \qquad (20)$$

Remarks

a) In the boundary layer $p=p_e(x_1,x_2)$. By using the physical gas equation (here the equation of perfect gas) the absolute temperature T inside the boundary layer can be expressed only in function of the pressure p_e at the edge and of ϱ i.e. $T = p_e/(\varrho\, R)$.

b) The viscosity μ depends only on the temperature T. If an exponential law is accepted and $\mu^*_\infty=\mu_\infty\ (\kappa/a^2_\infty)^n$ it results in:

$$\mu = \mu_\infty \left(\frac{T}{T_\infty} \right)^n = \mu^*_\infty \left(\frac{p_e}{\varrho} \right)^n \qquad (21)$$

c) The temperature T can be eliminated from the impulse equations (13a-c) and the partial differential equations of the three - dimensional compressible boundary layer can be splitted in two groups. The first one formed by the first four equations i.e. the continuity and the impulse equations, which depend on u_i, v_i, w_i and ϱ. The internal energy e is obtained from the equation (14a) in which the absolute temperature T is given from the physical gas equation. After these remarks the impulse equations written in $N_1=N-2$ chosen points P_k (k=1, 2, .. (N-2)) in the boundary layer are quadratic algebraic equations:

$$\sum_{i=1}^{N}\sum_{j=1}^{N} u_i(A^{(1)}_{ijk}\, u_j + B^{(1)}_{ijk}\, v_j + C^{(1)}_{ijk}\, w_j)$$
$$= A^{(1)}_{0k} + \sum_{i=1}^{N} (A^{(1)}_{ik}\, u_i + B^{(1)}_{ik}\, v_i + C^{(1)}_{ik}\, w_i)$$

$$\sum_{i=1}^{N}\sum_{j=1}^{N} v_i(A^{(2)}_{ijk}\, u_j + B^{(2)}_{ijk}\, v_j + C^{(2)}_{ijk}\, w_j)$$
$$= B^{(2)}_{0k} + \sum_{i=1}^{N} (A^{(2)}_{ik}\, u_i + B^{(2)}_{ik}\, v_i + C^{(2)}_{ik}\, w_i)$$

$$\sum_{i=1}^{N}\sum_{j=1}^{N} w_i(A^{(3)}_{ijk}\, u_j + B^{(3)}_{ijk}\, v_j + C^{(3)}_{ijk}\, w_j)$$
$$= \sum_{i=1}^{N} C^{(3)}_{ik}\, w_i \ . \qquad (22a\text{-}c)$$

The equations (22a-c) together with the boundary conditions (18a-c) and (19a-c) form a quadratic algebraic system with respect to the unknown coefficients u_i, v_i, w_i of u_δ, v_δ and w_δ. If δ and ϱ are firstly guessed in N_1 chosen points P_k in the boundary layer the 3N coefficients u_i, v_i, w_i can be obtained by solving the system given above. The remaining equations (20) and (12) (the last integrated once with respect on η) are used to correct ϱ and δ in the higher order iteration loops.

3. Computation of the Total Drag Coefficient $C_d^{(t)}$

The shear stress component $\tau^{(w)}_{x1}$ at the

wall and the friction coefficient $C_d^{(f)}$ are

$$\tau_{x_1}^{(w)} \equiv \tau_{x_1}\Big|_{\eta=0} = \mu \frac{\partial u_\delta}{\partial \eta}\Big|_{\eta=0} = \mu\, u_1\, u_e$$

$$C_d^{(f)} = 8\, \nu_f\, u_1 \int_{\tilde{0}\tilde{A}_1\tilde{C}} u_e\, \tilde{x}_1\, d\tilde{x}_1\, d\tilde{y} \qquad (23a,b)$$

The total viscous drag coefficient, is $C_d^{(t)} = C_d^{(f)} + C_d + C_d^*$. Hereby C_d and C_d^* are the inviscid drag coefficients of the thin and thick-symmetrical delta wing components given in (7a,b). In the (Fig.2) and (Fig.3) the total and the inviscid drag coefficients $C_d^{(t)}$ and $C_d^{(i)} = C_d + C_d^*$ and the polars of the wedged delta wing (Fig.1) are compared. The friction drag coefficient increases slower as the inviscid drag when the angle of attack increases. The spectral solutions are also very useful for the viscous optimal design.

4. The Optimal Aerodynamic Design of the Flying Configurations

The drag of the flying configurations FC at high speed (the supersonic aircraft, the waveriders and the space vehicles) can be very much reduced if the shapes of their surfaces are designed by performing a global optimization, i.e. their cambers, twists, and thicknesses distributions and also the similarity parameters of their planprojections are simultaneously optimized in order to reach a minimum drag at cruising Mach number. Additionally, the configuration must fulfill some local or global auxiliary conditions of geometrical, aerodynamical, thermal and structural nature. If an inviscid solution for the three-dimensional hyperbolic boundary value problem concerning the determination of the velocity field $\vec{v}$ is considered as start solution an inviscid optimal design is performed. The fully-optimized shape of the FC is obtained by using the Optimum - Optimorum Theory of the author in one step as in [1]-[13]. If more realistic viscous start software are used for the computation of the velocity field $\vec{v}$ the influence of viscosity in the total drag and in the fully-optimized shape of the FC can be obtained by using the Iterative Optimum-Optimorum Theory as in [13]-[18]. The author proposes her own three-dimensional zonal solutions (potential/boundary layer) as in [15],[18] as start solutions for the performing of the viscous optimal design of the shape of the FC. The inviscid and the viscous design of the delta wing alone are here performed as exemplification.

5. The Optimum-Optimorum Theory and the Inviscid Design

The optimum-optimorum theory allows the simultaneous determination of the optimal shapes of the surface and of the planprojection of the FC in order to obtain a minimum drag . The determination of the optimum-optimorum shape of the FC leads to an extended variational problem for the inviscid drag functional $C_d^{(i)}$, i.e.

$$C_d^{(i)} \equiv \int_{S(x_1,x_2)} F\left[\, x_1, x_2, Z(x_1,x_2)\right] dx_1\, dx_2 = \min. \qquad (24)$$

Here the function $Z(x_1,x_2)$ (i.e. the equation of the surface of the FC) and also the

boundary $S(x_1,x_2)$ of the integral (i.e. the similarity parameters of the planform of the FC) are a priori unknown and are determined by the solving of this extended variational problem. According to the Optimum-Optimorum Theory [2], [5] the optimum-optimorum FC is chosen among a set of admissible FC, which are defined through some common properties. In the frame of the author's optimum-optimorum theory, two FC belong to the same set if: their downwashes w and w^* (of the thin and thick-symmetrical components of the FC) can be piecewise approximated through two superpositions of homogeneous polynomes of the same degree; their planprojections are polygons which can be related through affine transformations and the shapes of the FC of the set fulfill the same auxiliary conditions (of geometrical or aerodynamical nature). The free parameters of the optimization are the coefficients $\tilde{w}_{ij}$ and $\tilde{w}^*_{ij}$ of the polynomial expansions of the downwashes w and w^*(i.e. of the local incidences and slopes of the surfaces) and the similarity parameters (ν_1, ν_2,..., ν_n) of the planprojections of the FC of the set.

In order to solve this enlarged variational problem for the determination of the extremum of the drag functional $C_d^{(i)}$ with free boundary the author uses her hybrid, numerical-analytical method. This method starts with the remark, that the dependence of the drag functional $C_d^{(i)}$ versus the coefficients $\tilde{w}_{ij}$ and $\tilde{w}^*_{ij}$ of these polynomial expansions of w and w^*, which piecewise approximate the incidences and the slopes of the surfaces of the FC, is quadratical while the dependence versus the similarity parameters ν_i of the planform is strong non-linear. The method presents two steps. In the first step the set of similarity parameters of the planform (ν_1, ν_2,..., ν_n) is considered as given. The boundary of the drag functional $C_d^{(i)}$ is now a priori known. The optimal values of the coefficients $\tilde{w}_{ij}$ and $\tilde{w}^*_{ij}$ of the downwashes w and w^* on the FC are obtained by solving a linear, algebraic system. These optimal coefficients determine uniquely the drag functional's value $(C_d^{(i)})_{opt}$, for the prescribed set of similarity parameters of the planform. This value of $(C_d^{(i)})_{opt}$ represents a "point" of what is called here lower limit hypersurface of the drag functional $C_d^{(i)}$

$$(C_d^{(i)})_{opt} = f(\nu_1, \nu_2,..., \nu_n) \qquad (25)$$

Each of these points is analytically determined by solving a classical variational problem with a given shape of the planform.In the second step, through systematical variation of the set of similarity parameters the "position" of the minimum of this hypersurface is numerically (or graphically) determined and gives the best set of similarity parameters (ν_1, ν_2,..., ν_n) of the planform. The optimal set of the similarity parameters together with a chosen area S_0 of the planprojection determine the shapes of the planform of the optimum-optimorum FC. The shape of the optimum-optimorum FC is the optimal FC corresponding to this optimal set of similarity

parameters. The minimum value of the "ordinate" of the hypersurface represents the drag coefficient of the optimum-optimorum FC of the set. The resulting Global Optimized Shape of the Configuration obtained by using the Classical Optimum-Optimorum Theory depends on the chosen "start" software for the calculation of the velocity field $\vec{v}$ around the configuration and on the chosen set of auxiliary conditions. The Optimum Optimorum Theory can be used for any set of auxiliary conitions and for any start software for $\vec{v}$.

In our previous papers we have used our own potential solutions as start solutions for $\vec{v}$ and a set of auxiliary conditions of geometrical and aerodynamical nature for the design of the Inviscid Fully-Optimized Shapes of the following three different flying configurations i.e.: the Delta Wing Alone, presented in (Fig. 4),and (Fig. 5a), and in [2]-[7], the Integrated Delta Wing-Fuselage Configuration presented in (Fig. 5b), and in [7]-[9] and the Integrated Delta Wing Fuselage-Leading Edge Flaps Configuration of Variable Geometry presented in (Fig. 5b,c) optimized at two, very different cruising Mach numbers M_∞^* and M_∞ ($M_\infty^* < M_\infty$) as in [10]-[13], [17]. At the higher supersonic Mach number M_∞ the integrated FC is flying with the flaps in retracted position as in (Fig. 5b). At the lower supersonic Mach number M_∞^* the FC is flying with the flaps in open position as in (Fig. 5c). The author proposes as in (Fig. 5a-c) the fully-optimized delta wing alone as the shape for the unmanned space vehicle, the integrated, fully-optimized, wing-fuselage configuration for the supersonic transport aircraft of second generation and for the both vehicles of the Sänger space vehicle in two stages and the integrated, fully-optimized wing-fuselage configuration of variable geometry (i.e. with movable leading edge flaps) for the single-stage space vehicle (like Hotol, Hermes and NASP). The effective design of the optimum-optimorum shape of the delta wing model Adela given in (Fig. 4) and of the integrated wing-fuselage model Fadet given in (Fig.5b) was performed by the author at cruising Mach number $M_\infty=2$ as in [2]-[7] and in [7]-[13]. The modification of the shape of the surface, due to the fuselage integration (in the section $\tilde{x}_1 = 0{,}6$) is obtained through comparison of the (Fig. 5a,b).

6. The Iterative Optimum-Optimorum Theory and the Viscous Design

If the more realistic viscous start software for the computation of the velocity field $\vec{v}$ is used and supplementary auxiliary conditions of thermal and structural nature are considered it is too complicate to use the Optimum-Optimorum Theory In One Step because the shape of its surface and of its planprojection are a priori unknown.

Therefore an Iterative Optimum-Optimorum Theory is here proposed. The Inviscid Optimum-Optimorum Shape of the Configuration, which uses an inviscid flow field (i.e. the full-linearized, full-potential, or Euler equations) as start solution for the optimization, represents now the First

Step in the iterative shape-optimization process. An Intermediate Computational Checking of the Inviscid Fully-Optimized Shape is introduced before the second step of the optimization is performed.The checking is made with a viscous solver (here a zonal potential/three-dimensional boundary layer). The shear stress coefficient τ_w on the wall and the global friction coefficient $C_d^{(f)}$ on the surface of the configuration are determined. The influence of temperature is also introduced in the computation of the viscosity coefficient μ. The inviscid fully-optimized shape is checked also for the thermal and structural point of view. This checking gives us realistic suggestions for the <Corrections> of the inviscid fully-optimized shape in the second optimization step. New local or global auxiliary conditions introduced for thermal, structural or boundary layer reasons can occur as for example a local limitation in the minimal thickness (for structural reasons) or limitation in the magnitude of curvature of the wing(in order to avoid great thermal gradients or some detachments of boundary layer). In the second step of optimization the predicted inviscid optimized shape of the configuration (obtained in the first optimization step) is corrected by including supplementary auxiliary conditions(for thermal and structural nature)in the variational problem and of the friction coefficient in the drag functional. The Iterative Optimization Process is repeated until the maximal local modification of the shape in two consecutive optimization steps presents no significant change. The author uses a zonal potential/boundary layer starting solver in order to correct the inviscid fully-optimized shape by taking into account the effect of viscosity as an exemplification of her Iterative Optimum-Optimorum Theory.

7. The Inviscid Design of the Delta Wing Alone

Let us suppose that the downwashes $\tilde{w}$ and $\tilde{w}^*$ of the thin and thick-symmetrical wing components of the thick, lifting delta wing are given in the form of superposition of homogeneous polynomes in $\tilde{x}_1$ and $\tilde{x}_2$ as in formulas (1a) and(1b),but in the design, the coefficients w_{ij} and w^*_{ij} and the similarity parameter ν of the planform are unknown and must be determined after the performing of the optimization process. The corresponding axial disturbance velocities u and u^* for the delta wing components with subsonic leading edges are given in the formulas (2), and (3) as in [1]-[7]. The coefficients $\tilde{a}^{(n)}_{2q,j}$, $\tilde{c}^{(n)}_{2q,j}$, $\tilde{h}^{*(n)}_{qj}$, $\tilde{d}^{*(n)}_{2q,j}$, $\tilde{c}^{*(n)}_{2q,j}$ entering in the formulas (5a,b) and (6a-c) are non-linear functions only of the unknown similarity parameter ν. Let us firstly perform the inviscid design of the delta wing as in [1]- [7] and in (Fig. 4). The optimal values of the coefficients $\tilde{w}_{ij}$ and $\tilde{w}^*_{ij}$ and of the similarity parameter ν of the planprojection are determined by using the own hybrid numerical-analytical method described in [1]-[7]. The optimal shape of the skeleton surface for a given value of ν is obtained by setting the drag functional

$$C_d \equiv \ell \sum_{n=1}^{N} \sum_{m=1}^{N} \sum_{k=0}^{m-1} \sum_{j=0}^{n-1} \tilde{\Omega}_{nmkj}\, \tilde{w}_{m-k-1,k}$$

$$\tilde{w}_{n-j-1,j} = \min. \qquad (26)$$

with the following auxiliary conditions:
-the lift coefficient C_ℓ is given:

$$\tilde{C}_\ell \equiv \sum_{n=1}^{N} \sum_{j=0}^{n-1} \tilde{\Lambda}_{nj}\ \tilde{w}_{n-j-1,j} = \frac{C_{\ell_0}}{\ell} \qquad (27)$$

- the Kutta condition on subsonic leading edge (i.e. $\tilde{u}_{\tilde{y}\to 1} = 0$) is fulfilled, in order to suppress the induced drag at cruising Mach number M_∞ i.e.

$$\tilde{F}_n \equiv \sum_{j=0}^{n-1} \tilde{\Psi}_{nj}\ \tilde{w}_{n-j-1,j} = 0 \qquad (28)$$

$(n = 0, 1,..., (N-1))$.

The coefficients $\tilde{w}_{ij}$ and the values of Lagrange's multipliers $\lambda^{(1)}$ and λ_n are given by the solving of the algebraic system as in [1]-[7] :

$$\sum_{n=1}^{N} \sum_{j=0}^{n-1} \left[\tilde{\Omega}_{n,\theta+\sigma+1,\sigma,j} + \tilde{\Omega}_{\theta+\sigma+1,n,j,\sigma} \right] \tilde{w}_{n-j-1,j} + \lambda^{(1)}\ \tilde{\Lambda}_{\theta+\sigma+1,\sigma} + \lambda_{\theta+\sigma+1}\ \tilde{\Psi}_{\theta+\sigma+1,\sigma} = 0, \qquad (29)$$

$(1 < \theta + \sigma + 1 < N\ ,\ \theta = 0,1,..., (N-1))$

Similarly, the optimal shape of the surface of the thick-symmetrical delta wing component is obtained by setting the corresponding drag functional

$$C_d^* = \ell \sum_{n=1}^{N} \sum_{m=1}^{N} \sum_{k=0}^{m-1} \sum_{j=0}^{n-1} \tilde{\Omega}^*_{nmkj}\ \tilde{w}^*_{m-k-1,k} \cdot \tilde{w}^*_{n-j-1,j} = \min. \qquad (30)$$

with the following auxiliary conditions:
the given relative volume

$$\tilde{\tau}^* \equiv \sum_{m=1}^{N} \sum_{k=0}^{m-1} \tilde{\tau}^*_{mk}\ \tilde{w}^*_{m-k-1,k} = \tau_0 \sqrt{\ell}$$

$(\tau_0 = V_0 / S_0^{3/2})$ (31)

the cancellation of the thickness along the leading edge

$$\tilde{E}^*_t \equiv \sum_{m=t+1}^{N} \sum_{k=0}^{m-1} \tilde{d}^{*(t)}_{mk}\ \tilde{w}^*_{m-k-1,k} = 0$$

$(t = 0, 1,..., (N-1))$. (32)

The coefficients $\tilde{w}^*_{ij}$ and the values of Lagrange's multipliers $\mu^{(1)}$ and μ_t are given by the solving of the algebraic system as in [1]-[7]:

$$\sum_{n=1}^{N} \sum_{j=0}^{n-1} \left[\tilde{\Omega}^*_{n,\theta+\sigma+1,\sigma,j} + \tilde{\Omega}^*_{\theta+\sigma+1,n,j,\sigma} \right] \tilde{w}^*_{n-j-1,j} + \mu^{(1)}\ \tilde{\tau}^*_{\theta+\sigma+1,\sigma} + \sum_{t=0}^{N-1} \mu_t\ \tilde{d}^{*(t)}_{\theta+\sigma+1,\sigma} = 0. \qquad (33)$$

$(1 < \theta + \sigma + 1 < N\ ,\ \theta = 0, 1,.., (N-1))$

The equations (29) and (33) are coupled through the parameter ν which enters in the constants of u and u^*. The hybrid numerical-analytical method (graphical-analytical) of the author as in [1]-[7] allows the numerical decoupling of these equations which are strongly non-linear in ν. Instead to solve a non-linear system a cascade of linear systems obtained by giving several discrete values to ν (between 0 and 1) are solved. The lower-limit curve of $(C_d^{(i)})_{opt}$ of the optimal inviscid drag introduced by the author as in [1]-[7] is obtained i.e.

$$(C_d^{(i)})_{opt} = f(\nu) \ . \qquad (34)$$

Each point of this curve is analytically determined by solving a classical variational problem with given boundary (i.e. given ν). The minimum of this curve is numerically determined. The position of this minimum drag represents the optimal value of ν ($\nu = \nu_{opt}$). If ν_{opt} is introduced in the equa-

tions (29), (33) the best values of $\tilde{w}_{ij}$ and $\tilde{w}^*_{ij}$ are obtained. These coefficients of w and w^*, together with a free chosen surface S_0 of the planprojection, determine the optimum-optimorum inviscid shape of the surface and of the planprojection of the delta wing as in (Fig. 4).

8. The Viscous Design of the Delta Wing Alone

Let us here perform the intermediate computational checking of the inviscid fully-optimized shape of the delta wing. This checking is made with a viscous solver.The own spectral solution for the three-dimensional boundary layer is here chosen. This checking is performed as in (Fig.6) and paragraph 3 i.e. ρ, $\tilde{\delta}^+_{ij}$ and $\tilde{\delta}^-_{ij}$ are, at the beginning, guessed. The coefficient $\tilde{w}^{(1)}_{ij}$ and $\tilde{w}^{*(1)}_{ij}$ are computed with the formulas (10a,b). In these formulas w_{ij} and w^*_{ij} are the optimized values determined by using the inviscid solver as in (29), (33), (34). The thicknesses δ^+ and δ^- of the boundary layer are obtained by using the formulas (8a), (8b). The edge axial velocities u_e and u^*_e are obtained from the formulas (2) and (3) in which the modified coefficients $\tilde{A}^{(1)}_{n,2q}$, $\tilde{H}^{*(1)}_{nq}$ etc. are obtained by replacing of w_{ij} and w^*_{ij} with $w^{(1)}_{ij}$ and $w^{*(1)}_{ij}$. The coefficients u_i, v_i, w_i of the velocities in the boundary layer are obtained by the solving of the quadratical algebraic system (22a-c) and ρ, δ_{ij} and δ^*_{ij} are corrected with the formulas (20) and (12). The global friction coefficient $C_d^{(f)}$ is computed with the formula (23b) and the new modified functional including the viscous effect is:

$$C_d^{(t)} = C_d^{(f)} + C_d + C_d^* \quad . \tag{35}$$

Hereby are C_d and C_d^* the inviscid drag coefficients of the thin and thick-symmetrical wing components given in (7a,b) and $C_d^{(f)}$ is the friction coefficient. The optimized shape of the delta wing obtained after the performing of the first iteration of the viscous design presents non-significant change (except on its rear part where it is thicker than the inviscid one) but the total drag (35) increases with 40% (at $M_\infty = 2$ and $\alpha = 0$) due to the viscous effect.

REFERENCES

[1] Nastase, A.,Utilizarea Calculatorelor in Optimizarea Formelor Aerodinamice, Ed.Acad.Romana 1973.

[2] Nastase,A.,The Design of Optimum-Optimorum Shapes of Aerodynamic Configurations, Mainz Printing House, Aachen, Germany, 1994, 300 p.

[3] Nastase, A.,Eine graphisch-analytische Methode zur Bestimmung der Optimum-Optimorum Form des dünnen Deltaflügels in Überschallströmung, R.R.S.T.-S.M.A., 1, 19, 1974.

[4] Nastase, A.,Eine graphisch-analytische Methode zur Bestimmung der Optimum - Optimorum Form des symmetrisch-dicken Deltaflügels in Überschallströmung, R.R.S.T.-S.M.A., 2, 19, 1974.

[5] Nastase, A.,Die Theorie des Optimum-Optimorum Tragflügels im Überschall.ZAMM 57,1977.

[6] Nastase, A., New Concepts for Design of Fully-Optimized Configurations for Future Supersonic Aircraft. Proceedings of the 12. Congress of ICAS, 1980, Munich, Germany.

[7] Nastase, A., Wing Optimization and Fuselage Integration for Future Generation of Supersonic Aircraft. Israel Journal of Technology, Jerusalem 1985.

[8] Nastase, A., Computation of Fully - Optimized Wing-Fuselage Configuration for Future Generation of Supersonic Aircraft, Proceedings of IMSE 86, Hemisphere Publ. Corp., Washington D.C., 1986. (Ed. F. Payne, C. Corduneanu, A. Haji-Sheikh, T. Huang).

[9] Nastase, A., Optimum-Optimorum Integrated Wing-Fuselage Configuration for Supersonic Transport Aircraft of Second Generation,

Proceedings of 15th ICAS Congress, London, UK, 1986.

[10] Nastase, A., The Design of Optimum-Optimorum Shape of Space Vehicle, Proceedings of the First International Conference on Hypersonic Flight in the 21st Century (M.E. Higbea, J.A. Vedda Edit.), University of North Dakota, Grand Forks (1988).

[11] Nastase, A., The Design of Supersonic Aircraft and Space Vehicles by Using Global Optimization Techniques, Collection of Technical Papers ISCFD, Nagoya, 1989.

[12] Nastase, A., The Optimum-Optimorum Shape of the Space Vehicle of Variable Geometry of Minimum Drag at two Cruising Mach Numbers, Proceedings of High Speed Aerodynamics II , 1990 (Ed. A. Nastase).

[13] Nastase, A., Over the Design of Supersonic Aircraft and Space Vehicles of Minimum Drag in Supersonic and Hypersonic Flow, Proceedings of the Integral Methods in Science and Engineering 90, Hemisphere Publishing Corporation, Washington D.C., 1990 (Ed. F. Payne, C. Corduneanu, H. Sheikh, R. Wilson).

[14] Nastase, A., The Aerodynamic Design Via Iterative Optimum-Optimorum Theory,Proceedings of the IV. International Symposium on Computational Fluid Dynamics, Vol. III, California Davis (1991).

[15] Nastase, A., The Design of Fully - Optimized Configurations by Using the Iterative Optimum -Optimorum Theory, ZAMM 72 (1992).

[16] Nastase, A., The Determination of Hybrid Analytical-Numerical Solutions for the Three-Dimensional Compressible Boundary Layer Equations, ZAMM (73) 1993.

[17] Nastase, A., The Design of Fully-Integrated Shape of Intercontinental Supersonic Transport Aircraft of the Second Generation by Using the Global Optimization Techniques, ICAS - Proceedings 1990, Stockholm.

[18] Nastase, A., The Design of Fully-Integrated Shape of Waverider by Using Global Optimization Techniques, Proceedings of the First International Hypersonic Waverider Symposium, October 1990, University of Maryland,Washington D.C. (Ed. J.D. Anderson).

[19] Nastase, A., Spectral Solutions for the Three-Dimensional Boundary Layer and Their Application for the Optimal Viscous Design,Proceedings of the 5th International Symposium on Computational Fluid Dynamics, Tohoku University Sendai ,1993 (Edit. H. Daiguji).

[20] Young, A.D., Boundary Layers, Blackwell Scientifical Publications London, 1989.

[21] Schlichting, H., Boundary Layer Theory, Mc. Graw-Hill, 1979.

[22] Carafoli, E., Mateescu, D., Nastase, A., Wing Theory in Supersonic Flow, Pergamon Press, 1969, 500 p.

[23] Van Dyke, M., Perturbation Methods in Fluid Mechanics, Acad. Press, New York, (1964).

[24] Nastase, A., L'Etude du Comportement Asymptotique des Vitesses Axiales de Perturbation au Voisinage des Singularites, R.R.S.T.-M.A., 4, 17, (1972), (Romania).

FIGURES

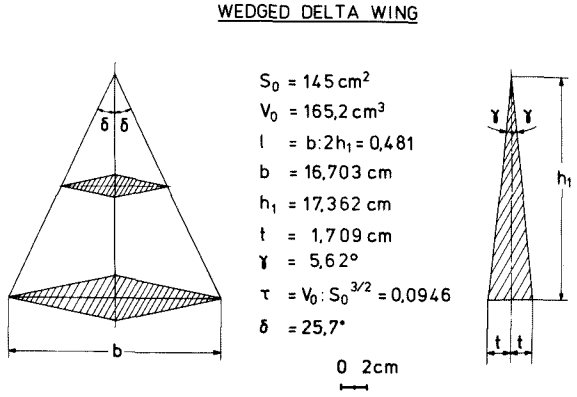

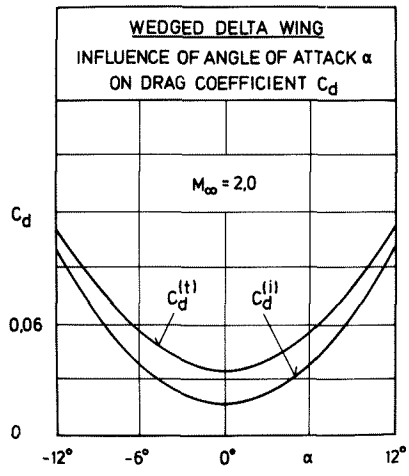

Fig. 1,2

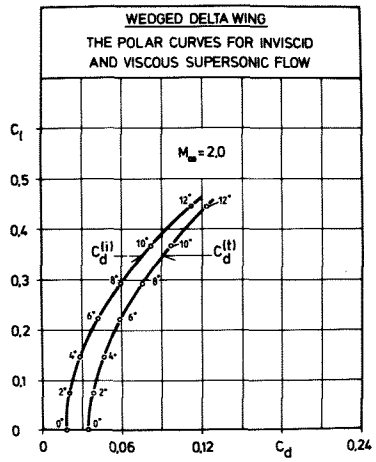

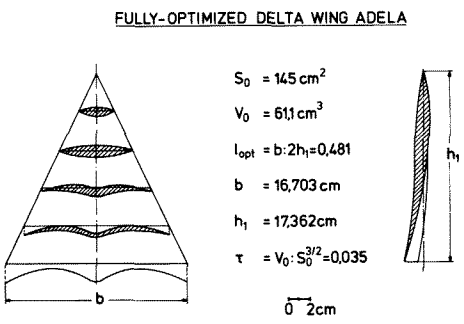

Fig. 3,4

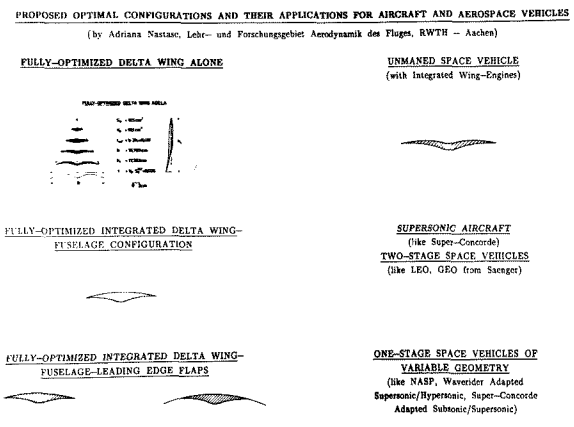

Fig. 5a-c

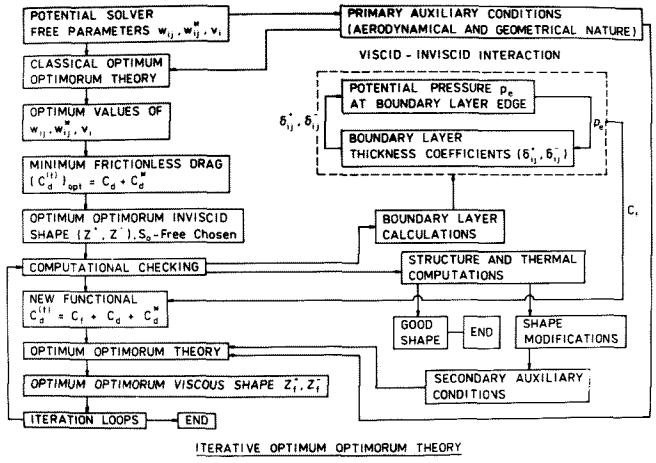

Fig. 6